



A11105 898767

NBS
PUBLICATIONS

NBSIR 81-2255

A Diffusive Crack Growth Model for Creep Fracture

Tze-jeer Chuang

Fracture and Deformation Division
National Measurement Laboratory
Center for Materials Science
U.S. Department of Commerce
National Bureau of Standards
Washington, DC 20234

March 1981

QC
100
.U56
81-2255
1981
c.2

for
Department of Energy
Washington, DC

JUL 20 1981

Not on file - Curran

Oct 1980

U.S.G.

No. 81-2255

1981

L. 80

NBSIR 81-2255

A DIFFUSIVE CRACK GROWTH MODEL FOR CREEP FRACTURE

Tze-jer Chuang

Fracture and Deformation Division
National Measurement Laboratory
Center for Materials Science
U.S. Department of Commerce
National Bureau of Standards
Washington, DC 20234

March 1981

Prepared for
Department of Energy
Washington, DC



U.S. DEPARTMENT OF COMMERCE, Malcolm Baldrige, *Secretary*
NATIONAL BUREAU OF STANDARDS, Ernest Ambler, *Director*

A DIFFUSIVE CRACK GROWTH MODEL FOR CREEP FRACTURE

TZE-JER CHUANG

Fracture and Deformation Division
National Bureau of Standards
Washington, D.C. 20234

Filed 1-5-81
~~October 1980~~

ABSTRACT

A grain boundary creep crack growth model is presented here based on the assumptions that the crack propagates along the grain boundary by a coupled process of surface and grain-boundary self-diffusion; the adjoining grains on either side of the boundary do not behave plastically; and steady state conditions prevail. Under the action of the applied stress atoms on the crack surfaces are driven by surface diffusion toward the crack tip from where they are deposited non-uniformly by grain-boundary diffusion along the grain interface so that the grain boundary opens up in a wedge shape ahead of the advancing tip which in turn produces a misfit residual stress field. The total grain boundary normal stresses which are the sum of this misfit stress field and that due to applied stress as well as the boundary opening displacements due to materials deposition are solved from a singular integro-differential equation to give the following equation relating K to v :

$$K/K_{\min} = \frac{1}{2} [(v/v_{\min})^{1/12} + (v/v_{\min})^{-1/12}]$$

where K is the mode I crack tip stress intensity factor, $K_{\min} = 1.69 K_G$ is the minimum K below which no crack growth is predicted, K_G being the stress intensity based on the Griffith theory; v is the stationary crack tip velocity and v_{\min} is the minimum v for which $K = K_{\min}$. In terms of the conventional expression of $v \propto K^n$, the present model predicts the values of n varying from 12 to infinity. A comparison with a set of creep crack growth data on Si-Al-O-N at 1400 °C shows good agreement between the theory and experiment.

A detailed analysis of the energy balance for the present model is also presented which indicates J or $(1-v^2)K^2/E$ is indeed the correct energy release rate during the crack growth as is true in the theory of elastic fracture mechanics. However, the energy released in the diffusion processes is in the form of work done by the normal stress rather than in the form of elastic strain energy of the grains.

1. Introduction

At high temperatures grain boundary cavitation is a general phenomenon accompanying the process of creep rupture: cavity nuclei at the grain interfaces grow to coalesce with each other until the remaining ligament can no longer support the sustained loads and premature failure takes place. The prediction of time to fracture is thus important for the design of structural components subject to creep conditions. For materials such as ceramics where pores have been introduced at the boundaries in the process of fabrication prior to service, emphasis is given to the study of in-service cavity growth since nucleation plays only a minor role in the entire service life. Indeed, the subject of intergranular cavity growth has been under intensive research in the past few years. The cavity growth at elevated temperatures is generally believed to be controlled by surface and grain boundary self-diffusion since observations frequently revealed that a majority of the void population appears at the boundaries normal to the direction of the applied tensile stress, although other possible mechanisms such as grain sliding, dislocational slip, etc., may be in operation as well. The first model of cavity growth by diffusion was proposed by Hull and Rimmer [1] who considered a square array of spherical voids on a grain boundary slab normal and subject to a tensile load. It was found that the void growth rate increases linearly with increasing applied stress assuming the grains on both sides of the boundary are rigid. Raj and Ashby [2] considered a network of lenticular cavities and obtained a similar conclusion. Unfortunately, creep experiment data do not always agree with their predictions and optical metallographs often show that the morphology of intergranular voids look thin and crack-like, rather than spherical or lenticular, indicating that the quasi-equilibrium conditions at the void surface are

not always fulfilled. This case has been considered by Chuang and Rice [3] who found the near tip void profile during the steady state growth. In an overview of the subject, Chuang et al. [4] investigated the time-dependent aspect of the problem and obtained a class of "self-similar" solutions which indicate that initially cavities grow slowly in a quasi-equilibrium shape which gradually becomes crack like as the propagation rate increases. A growth rate parameter was identified which sets the transition period between these two extreme modes. In general, the crack like growth mode prevails when the applied stress, the cavity size, and the grain boundary diffusivity are large as compared to the capillarity stress, the cavity spacing, and the surface diffusivity. The equilibrium shape is favored by the opposite situation.

The present paper restricts the discussion to the limiting case of crack like cavity growth in steady state as opposed to another extreme case of Hull-Rimmer type cavities. The central issue to be addressed in the present paper is "what is the sustained load required for a boundary crack to propagate at a given velocity and temperature for a known material?" Mathematically this means that a functional relationship between the applied stress and the crack tip velocity has to be formulated. In the circumstances, this can be regarded as an extension of work that was originated by Chuang and Rice [3].

This problem has been well treated in cases where the separation between the adjacent cracks is so close that the adjoining grains essentially behave rigidly. However, if the neighboring cracks are remotely apart or if a main crack is growing in isolation, the grain deformability becomes important and therefore must be taken into account. Previous attempts to model the combined effects of elastic deformation and diffusion on crack

growth were made by Vitek [5] and Speight et al. [6]. In the former model, an enforcement that the crack maintains a constant thickness during the growth regardless of the level of the applied stress is imposed while in the latter model, a parabolic distribution of the boundary displacements in a "wedge" shape ahead of the running crack tip is assumed. Further, the near tip void shape is not analyzed in detail. As a consequence, the crack tip conditions together with the related physical laws, as will be discussed later, are either not satisfied or satisfied only in approximation. In contrast, our work attempts to solve exactly the coupled problem of elasticity and diffusion so that both grain boundary stresses and displacements are determined as part of the solution. As will be seen, the end results regarding the functional dependence of the applied stress on the crack growth velocity are quite different although some similar features are exhibited.

The program of the paper is as follows: In section 2 we present the self-consistent model of steady state growth, beginning with descriptions of the mathematical model from which control equations and boundary conditions at the advancing crack tip are derived based on certain justifiable physical assumptions. A unique solution is pursued and detailed elaborations leading to the expression of external loading intensity in terms of the crack growth rate are given in section 2.4. For a growing crack, it is well recognized that a portion of energy is released in the body during the growth. This energy provides a driving force causing the crack to grow. Hence in section 3 we present a detailed calculation on the energy release rate associated with our crack growth model. This promotes the analytical rigorousness of our model and provides physical insight as to how and where the energy dissipation takes place. A discussion follows in section 4 where a comparison between

the present theory and a set of creep test data on ceramics and comparisons with the other two models previously mentioned are presented. Finally, section 5 summarizes and gives conclusions drawn from the discussion presented. We conclude that whereas the other models proposed thus far possess some theoretical deficiencies, the current theory is developed in a self-consistent fashion. The excellent agreement between the theoretical predictions presented here and recent test data [7] obtained from creep experiments on Si-Al-O-N at 1400 °C points up a bright prospect. Hopefully, future creep tests on other ceramics will show similar features predicted by the current theory.

2. The Steady State Crack Growth Model

Before we enter into detailed elaborations on the proposed model, the physical process is given first by which the model is designed to represent the case of a creep crack growing in steady state at a fixed velocity, v , along a grain interface normal to an applied stress, σ_{∞} . As mentioned in section 1, the kinetics of the crack growth is assumed to be controlled by a coupled process of surface and grain boundary diffusion. Of course, at the crack surfaces lattice diffusion as well as evaporation and condensation may also play a role in the mass transport process whereas in the grain boundary bulk diffusion may drive atoms out of the boundary zone. However, it has been shown [4] that at least for the crack size (in the order of microns) and temperature range (between 0.3 to 0.8 T_m , T_m being the melting temperature in K) we consider here, surface diffusion and grain boundary diffusion are the dominate mechanisms at the surfaces of the crack and in the grain boundary, respectively. Hence atoms are driven along the crack wall by surface diffusion toward and into the crack tip from where grain boundary diffusion further carries them away along the grain boundary. The steady state is reached when all related physical parameters

become invariant with regard to an observer stationed at the advancing crack tip. The grains on both sides of the interface are considered homogeneous, isotropic, and linear elastic free of dislocations even in the near tip zone. This is a reasonable assumption for strong brittle materials such as ceramics where evidence indicates that the dislocations near the crack tip are essentially immobile [8] during the entire creep life. On the other hand, this assumption may not be valid for ductile materials such as metals where substantial dislocational creep might take place inside the grains especially in the vicinity of the crack tip [9]. Hence the current model has direct application to high temperature creep crack growth in ceramics.

2.1 Descriptions of the mathematical model

The limiting case of propagation of an isolated long boundary crack led us to consider an infinite bicrystal containing a semi-infinite crack colinear with a grain boundary line on the x_1 -axis subjected to a uniform tensile stress, σ_∞ applied remotely in the x_2 -direction and to a uniform temperature T as illustrated in figure 1. Under the action of σ_∞ , the crack tip is propagating at a constant velocity, v , in the positive x_1 -direction. A separate moving rectangular coordinate system of (x, x_2, x_3) with its origin coinciding with the advancing tip is also established so that $x = x_1 - vt$. The geometry has a long dimension in x_3 resulting in a two-dimensional problem with plane strain conditions. This is justified since the geometry of a long thin crack dictates that the principal curvature of its tip shape in the x_1 - x_2 plane is much larger than that of the crack front in the x_1 - x_3 plane. Accordingly, the two-dimensional plane strain conditions prevail and consideration of a unit length in the x_3 -direction is fully representative of the whole problem. Furthermore, the following

physical conditions are also assumed: (1) the crack surfaces are clean and free of traction (pressure) or environmental attack. In other words, the interior of the void is a vacuum, free of glassy or viscous phases; (2) the grain boundary is a perfect matter sink, capable of transporting material and is a flat slab of constant thickness constituting an effective diffusion zone; (3) the matrix of the bicrystal is a homogeneous, isotropic body composed of linear elastic material free of defects; (4) the composition remains unchanged at the surfaces and in the grain boundary during the entire period of the crack growth so that single-valued macroscopic chemical potentials of atoms can be defined in the diffusion process; and (5) the diffusional properties of material are isotropic, independent of temperature and crystal orientation.

This model configuration and physical assumptions are set to represent the limiting case of boundary cavitation in which the cavity has grown into a long crack-like shape and senses no effects from the neighboring defects.

2.2 Boundary conditions at the crack tip

Our goal is to pursue solutions for the distribution of the normal stress $\sigma(x)$ and opening displacement, $\delta(x)$, along the grain boundary and thereby correlate the applied stress, σ_∞ , or the crack tip stress intensity factor, K , with the crack velocity, v . It will become clear that the boundary conditions at the moving crack tip are required in order to do so. Those are derivable from the steady state crack tip shape solution obtained by Chuang and Rice [3]. The results are summarized in this section.

It is well known in diffusion theory that a non-uniform distribution of chemical potentials incurs an irreversible diffusional flux of matter. The chemical potential per atom at the surface is

$$\mu_s = -\Omega\gamma_s K \quad (1)$$

in relation to a reference state of flat surface where we arbitrarily set $\mu_s = 0$. Here Ω is atomic volume, γ_s surface free energy, and κ is the mean curvature of the surface at the point under consideration, assuming a positive sign for a concave surface. This expression results from the fact that there is no normal stress and the strain energy contributions associated with the surface stresses are small even at the crack tip and hence can be neglected [10,12]. The linearized theory of diffusion, known as Ficks law, calls for a linear dependence of matter flux on the gradients of the chemical potential, namely $J_s \propto -\nabla\mu$. This phenomenological law appears to be followed by nature, at least in the neighborhood of an equilibrium condition. For surface diffusion, the version of this equation is $\Omega J_s = -(D_s \delta_s / kT)(d\mu_s / ds)$ where ds is an element of arc length along the surface, D_s the surface diffusivity, and δ_s the thickness of the diffusion layer. Adopting $\delta_s = \Omega^{1/3}$ and substituting equation (1) one obtains

$$J_s = (D_s \gamma_s \Omega^{1/3} / kT) dk / ds \quad (2)$$

For a given rate of crack growth, the entire crack surface profile is obtained by solving the simultaneous equations of mass conservation and surface diffusion (Eq. (2)); the results show a constant crack thickness $2w$ proportional to $u^{-1/3}$ developed far away from the crack tip:

$$2w = 2\sqrt{2} (1 - \gamma_b / 2\gamma_s)^{1/2} (D_s \gamma_s \Omega^{4/3} / u k T)^{1/3} \quad (3)$$

where γ_b is the grain boundary free energy. The solution further indicates that approximately both surface flux and curvature decay exponentially with increasing S

$$\begin{pmatrix} J_s \\ \kappa \end{pmatrix} = \begin{pmatrix} (J_s)_{\text{tip}} \\ \kappa_{\text{tip}} \end{pmatrix} \exp(-\xi S) \quad (4)$$

where S = arc length along the crack surface measured from the crack tip; $dS = -ds$

$$\xi = (D_s \gamma_s \Omega^{4/3} / u k T)^{-1/3}$$

$(J_s)_{\text{tip}}$ = surface flux at the crack tip

$$= \sqrt{2} (1 - \gamma_b / 2\gamma_s)^{1/2} (D_s \gamma_s / k T \Omega^{5/3})^{1/3} u^{2/3} \quad (5)$$

K_{tip} = surface curvature at the point immediately adjacent to the crack tip

$$= \sqrt{2} (1 - \gamma_b / 2\gamma_s)^{1/2} (k T / D_s \gamma_s \Omega^{4/3})^{1/3} u^{1/3} \quad (6)$$

It should be noted here that all parameters summarized above including the crack shape are dependent on the applied stress since they are functions of u .

At the grain boundary, the chemical potential per atom is

$$\mu_b = -\sigma \Omega \quad (7)$$

where again we arbitrarily set $\mu_b = 0$ for a reference state in which $\sigma = 0$, σ being the normal tensile stress at the boundary acting in x_2 . Further, the strain energy term has been justifiably neglected [10,12].

In analogy to the case of surface diffusion, the version of Fick's law in grain-boundary diffusion is $\Omega J_b = -(D_b \delta_b / k T) d\mu_b / dx$. After substituting the expression of μ_b from Eq. (7), one obtains

$$J_b = \frac{D_b \delta_b}{k T} \frac{d\sigma}{dx} \quad (8)$$

where J_b is grain boundary atomic flux, D_b the grain-boundary diffusivity and δ_b the effective thickness (assume constant for simplicity) of diffusion zone in the grain boundary.

At the crack tip where the two crack surfaces join the grain boundary the following conditions have to be met:

$$(\mu_s)_{\text{tip}} = (\mu_b)_{\text{tip}} ; \quad (9a)$$

$$2(J_s)_{\text{tip}} = (J_b)_{\text{tip}} . \quad (9b)$$

Eq. (9a) follows from the requirement of continuity in chemical potentials and Eq. (9b) from conservation of mass. By means of these two equations the expressions of $(J_s)_{\text{tip}}$ and $(\kappa)_{\text{tip}}$ in Eqs. (5) and (6) can be transferred as follows to a more useful form. First we observed that after substitution of Eqs. (1) and (7) in Eq. (9a), $-\kappa_{\text{tip}} \gamma_s \Omega = -\sigma_{\text{tip}} \Omega$ from which we find

$$\sigma_{\text{tip}} = \sigma(0) = \sqrt{2}(1-\gamma_b/2\gamma_s)^{1/2} (kT\gamma_s^2/D_s\Omega^{4/3})^{1/3} u^{1/3} \quad (10)$$

Second, the grain boundary diffusion equation of Eq. (8) evaluated at the crack tip ($x = 0$) is $(J_b)_{\text{tip}} = D_b \delta_b \sigma'_{\text{tip}} / kT$ where $\sigma'_{\text{tip}} = d\sigma/dx \Big|_{x=0}$. It follows from Eqs. (9b) and (5) that

$$\sigma'_{\text{tip}} = 2 \sqrt{2}(1-\gamma_b/2\gamma_s)^{1/2} [(D_s\gamma_s)^{1/3} (kT)^{2/3} / D_b \delta_b \Omega^{5/7}] u^{2/3} \quad (11)$$

Eqs. (10) and (11) show that the normal stress and its derivative in x at the crack tip are in proportion to $u^{1/3}$ and $u^{2/3}$, respectively. Both equations will be seen useful as boundary conditions for future stress solutions.

2.3 Derivation of the field equations

The objective of this section is to derive the field equations governing the interaction of elasticity and diffusion from which the solution of stress can be obtained to predict the functional relationship between the stress intensity and the crack tip velocity. Specifically, emphasis will be placed on two parameters: the grain-boundary normal stresses, $\sigma(x)$, and opening displacements, $\delta(x)$.

As atoms on the crack surfaces diffuse into the grain boundary at the crack tip, the opening displacements of yet to be determined quantities, $\delta(x)$, along the g.b. are generated which in turn create a misfit residual stress field inside the grains and also along the grain boundary. However, our interests are restricted to the boundary line so that the relationship between $\delta(x)$ and $\sigma(x)$ can be formulated. We note that in the case of Griffith crack extension such as considered by Stevens and Dutton [11], no $\delta(x)$ is considered to take place and as a consequence the actual stress field is produced solely by the applied stress.

Steady state conditions require that $\delta(x) = \delta(x_1 - ut)$ so that $\partial\delta/\partial t = -u\partial\delta/\partial x$. In addition, for mass conservation in the boundary, $\partial\delta/\partial t = -\Omega\partial J_b/\partial x$ must be satisfied. Both conditions lead to $u\delta/dx = \Omega dJ_b/dx$. But physically both δ and J_b must decay to zero as x approaches infinity. Thus

$$\delta(x) = \frac{\Omega}{u} J_b(x) \quad (12a)$$

At the crack tip we find

$$\delta_{\text{tip}} = \delta(0) = \frac{\Omega}{u} (J_b)_{\text{tip}} = 2w \quad (12b)$$

according to Eqs. (3), (5), and (9b).

Finally, we find the relation between δ and σ from Eqs. (8) and (12a)

$$\delta(x) = \frac{D_b \delta_b \Omega}{u k T} \frac{d\sigma}{dx} \quad (13)$$

which means the $\delta(x)$ are in direct proportion to $\sigma'(x)$.

To evaluate the residual stress field generated by the unknown, a priori distribution of $\delta(x)$, we found it useful to employ the concept of infinitesimal dislocation theory in mathematics.

Consider an edge dislocation of Burgers vector, b , located at $x = x'$ on the grain boundary as shown in figure 2a. The residual misfit stress, $\sigma_m(x)$, introduced by this dislocation at an arbitrary distance, x on the grain boundary (x coordinate line) is [10]

$$\sigma_m(x) = \frac{Eb}{4\pi(1-\nu^2)(x-x')} \sqrt{\frac{x'}{x}} \quad (14)$$

where E is Young's modulus and ν Poissons ratio. This equation was derived based on the physical assumption (3) in section 2.1, and obtained by superposition of the stress field induced by the dislocation at $x = x'$ (figure 2b) and that created by dislocational image forces acting along the crack lines (figure 2c). The resultant two-dimensional stress field thus not only satisfies the equilibrium and compatibility equations throughout the whole body but also yields the free traction forces at the outer boundaries at infinity as well as along the crack line.

Now, imagine that the opening displacements along the grain boundary are due to a continuous distribution of infinitesimal edge dislocations in the grain boundary so that $b = -(\partial\delta/\partial x)dx$ being the total Burgers vector lying between x and $x + dx$. Then the residual stress induced by the non-uniform distribution of δ over the whole grain boundary is given by integration of Eq. (14). Thus

$$\sigma_m(x) = \frac{E}{4\pi(1-\nu^2)} \int_0^{\infty} \frac{\delta'(x')}{x'-x} \sqrt{\frac{x'}{x}} dx' \quad (15)$$

Here, $\delta'(x')$ denotes $d\delta(x')/dx'$ and the integration is performed in the sense of Cauchy principal value.

To evaluate the total stress of the grain boundary we first observed that, in the absence of diffusion, the stress field created by the external loads has a standard characteristic singularity of $r^{-1/2}$ (where r is the radial distance from the crack tip) as predicted by Irwin-Williams fracture mechanics theory. Then applying the well-known superposition principle in the theory of linearized elasticity the actual stress at an arbitrary location x on the grain boundary is

$$\sigma(x) = \frac{K}{\sqrt{2\pi x}} + \frac{E}{4\pi(1-\nu^2)} \int_0^{\infty} \frac{\delta'(x')}{x'-x} \sqrt{\frac{x'}{x}} dx' \quad (16)$$

where K is the crack tip stress intensity factor. The first term on the right hand side of Eq. (16) is due to the applied loads and the second term is that back stress generated by matter previously diffused from the crack surfaces.

Eqs. (13) and (16) are the field equations derived for the two unknown variables, δ and σ , based on the linearized theories of elasticity and diffusion. These simultaneous equations, together with boundary conditions at the crack tip, Eqs. (10) and (11) are to be solved in the following section.

2.4 The numerical solution

In this section we present solutions to simultaneous Eqs. (13) and (16) subjected to initial conditions (10) and (11) derived in sections 2.2 and 2.3. After a careful study, it is found that this system of differential equations is difficult to solve analytically and a numerical approach has to be adopted. To begin, we found some rearrangements and simplifications of the equations are quite useful. First, we note that δ can be temporarily

eliminated, thus reducing two equations to only one. This is done by substituting Eq. (13) in Eq. (16)

$$\sigma(x) = \frac{K}{\sqrt{2\pi x}} + \lambda \int_0^{\infty} \frac{\sigma''(x')}{x'-x} \sqrt{\frac{x'}{x}} dx' \quad (17)$$

where

$$\lambda = ED_b \delta_b \Omega / 4\pi(1-\nu^2)\nu kT.$$

This is a one-dimensional singular integro-differential equation of Cauchy type for $\sigma(x)$. To simplify, we apply the well known Cauchy inversion formula

[10] and observe that $\int_0^{\infty} [x'^{-1/2}/(x'-x)] dx' = 0$ for $x > 0$, Eq. (17) reduces

to the following simple form

$$L^2 \sigma''(x) = \int_0^{\infty} \frac{\sigma(x')}{x-x'} dx' \quad (18)$$

where

$$L = \left[\frac{\pi}{4} \frac{ED_b \delta_b \Omega}{(1-\nu^2)\nu kT} \right]^{1/2} \quad (19)$$

is a characteristic length depending on crack velocity, temperature, elastic and diffusional properties. Eq. (18) can be simplified further if we introduce the following non-dimensional variables

$$\hat{x} = x/L ; \hat{x}' = x'/L \text{ and } \hat{\sigma}(\hat{x}) = \frac{\sigma(x)}{\sigma_{\text{tip}}} \quad (20)$$

Then Eq. (18) becomes

$$\hat{\sigma}''(\hat{x}) = \int_0^{\infty} \frac{\hat{\sigma}(\hat{x}')}{\hat{x}-\hat{x}'} d\hat{x}' \quad (21)$$

and the initial conditions, Eqs. (10) and (11) take the following simple form

$$\hat{\sigma}(0) = 1 \quad (22a)$$

$$\hat{\sigma}'(0) = \alpha \quad (22b)$$

where

$$\alpha \equiv \sigma'_0 L / \sigma_0 = \sqrt{\pi E / (1-\nu^2)} D_s^{2/3} \Omega^{7/18} / [(D_b \sigma_b)^{1/2} \gamma_s^{1/3} (\nu k T)^{1/6}] \quad (23)$$

Equation (23) is obtained by substitution of expressions of σ_0 , σ'_0 , and L from Eqs. (10), (11), and (19).

Equations (21) and (22) constitute a well-defined initial value problem readily solved by numerical method. However, at $\hat{x} = \hat{x}'$ the singularity in the integral creates problems in the course of numerical integration. It is found that the singularity can be removed by integration by parts twice for the integral provided that the stress curve over the whole range $(0, \infty)$ satisfies the following conditions: (1) $\hat{\sigma}(\hat{x})$ be continuous, (2) $\hat{\sigma}'(\hat{x})$ be bounded, and (3) $\hat{x}^{1/2} \hat{\sigma}$ remains stationary as \hat{x} approaches infinity. It will be seen that these are reasonable assumptions and the final solutions do meet these conditions. The final result is

$$\psi(\hat{x}) = f(\hat{x}) + \int_0^{\infty} K(\hat{x}-\hat{x}') \psi(\hat{x}') d\hat{x}' \quad (24)$$

where ψ is the second derivative of stress, f is a given function of \hat{x} , and $K(\xi)$ is the kernel of the integral equation defined as follows

$$\psi(\hat{x}) = \hat{\sigma}''(\hat{x}) \quad (25a)$$

$$f(\hat{x}) = \ln \hat{x} + \alpha \hat{x}(\ln \hat{x} - 1) \quad (25b)$$

$$K(\hat{x} - \hat{x}') = (\hat{x} - \hat{x}')[\ln|x - \hat{x}'| - 1] \quad (25c)$$

Eq. (24) becomes a regular Fredholm-type integral equation, free of singularities although the upper integration limit extends to infinity and the function $f(\hat{x})$ has a logarithmic singularity at $\hat{x} = 0$. Detailed procedures of solving Eq. (24) are given in the Appendix. The end results are presented here. First of all, it is clear that for a given α there exists a corresponding solution for ψ (and hence for σ). Figure 3 illustrates two typical solutions of ψ for $\alpha = 0$ and 20, respectively. The feature of logarithmic singularity at the crack tip is observed. The stress $\hat{\sigma}$ can be obtained by integration of ψ twice subject to the initial conditions in Eqs. (22). Before we do so, observe that the integral equation (24) dictates a linear dependence of ψ (and hence $\hat{\sigma}$) on α , accordingly it is convenient to express $\hat{\sigma}$ in terms of the following form

$$\hat{\sigma}(\hat{x}) = \hat{\sigma}_0(\hat{x}) + \alpha \Delta \hat{\sigma}(\hat{x}) \quad (26)$$

where $\hat{\sigma}_0$ denotes solution of $\hat{\sigma}$ for $\alpha = 0$ and $\Delta \hat{\sigma} = \hat{\sigma}_1 - \hat{\sigma}_0$ represents the difference between solutions for $\alpha = 1$ and 0. Figure 4 shows the basic solutions of $\hat{\sigma}_0$, $\hat{\sigma}'_0$, $\Delta \hat{\sigma}$, and $\Delta \hat{\sigma}'$ obtained by integrating figure 3 with the aid of Eqs. (22) and (26). It can be seen that the maximum value of $\Delta \hat{\sigma}$ is at $\hat{x} = 0.9$ which implies that the peak stress for any α cannot occur beyond the region for which $x > 0.9L$. With the availability of figure 4, the solutions for δ and $\hat{\sigma}$ at any value of α can be obtained by the help of Eq. (26). To obtain the distributions of δ , we find from Eqs. (13) and (26) that

$$\delta = (\hat{\sigma}'_0/\alpha) + \Delta \hat{\sigma}' \quad (26-1)$$

where $\delta = \delta/\delta_{tip}$ is the nondimensional grain boundary opening displacement normalized against δ_{tip} . Using this equation to assemble the curves of δ

from $\hat{\sigma}'_0$ - and $\Delta\hat{\sigma}'$ curves given in figure 4, figure 5 illustrates typical solutions of δ for $\alpha = 1, 2, 5, 10,$ and ∞ , respectively. It is shown that the grain boundary opens up ($\delta > 0$) in the near tip region where $\hat{x} < 1$; elsewhere along the grain boundary, the δ is negative implying close-up of the boundary zone.

Similarly from the curves of $\hat{\sigma}$ and $\Delta\hat{\sigma}$ shown in figure 4, the stress solutions can be assembled for any α according to Eq. (26). Figure 6 gives some typical curves of $\hat{\sigma}$ for various values of α . As predicted, the peak stress approaches asymptotically to the line of $\hat{x} = 0.9$ as α becomes larger and larger.

The mode I crack tip stress intensity factor, K , is obtained by taking the limiting value of ψ or $\hat{\sigma}$ as \hat{x} approaches infinity. Of course, K is linearly dependent on α . From the standpoint of numerical evaluation, the value of K given by solution of ψ is more accurate than that given by $\hat{\sigma}$ in practice. A fuller discussion is included in the appendix. The final result is

$$K = 0.75 \sigma_{\text{tip}} L^{1/2} + 0.60 \sigma'_{\text{tip}} L^{3/2} \quad (27)$$

After substitution of σ'_{tip} , L , and σ_{tip} from Eqs. (11), (19), and (10) we obtain

$$K = A\nu^{1/12} + B\nu^{-1/12} \quad (28a)$$

where

$$A = 1.00 (1-\gamma_b/2\gamma_s)^{1/2} [\gamma_s^{2/3} (KT)^{1/12} D_s^{-1/3} \Omega^{-7/36}] [ED_b \delta_b / (1-\nu^2)]^{1/4} \quad (28b)$$

$$B = 1.42 (1-\gamma_b/2\gamma_s)^{1/2} [\Omega^{7/36} (D_s \gamma_s)^{1/3} (D_b \delta_b)^{-1/4} (KT)^{-1/12}] [E/(1-\nu^2)]^{3/4} \quad (28c)$$

A plot of K vs ν for Eqs. (28) exhibits a cut-off point below which no crack growth is expected. Denoting the values of K and ν for this point as K_{min} and ν_{min} , one obtains from Eqs. (28)

and

$$v_{\min} = (B/A)^6 = 8.13 D_s^4 \Omega^{7/3} [E/(1-\nu^2) D_b \delta_b]^3 / K T \gamma_s^2 \quad (29a)$$

where

$$K_{\min} = 2\sqrt{AB} = 1.69 K_G \quad (29b)$$

$$K_G = \sqrt{E(2\gamma_s - \gamma_b)/(1-\nu^2)} \quad (29c)$$

is the K value predicted by the Griffith theory for propagation of an atomistically sharp crack in an interface. It asserts that the energy release rate must be balanced by the net increase of the surface energy due to an infinitesimal increase in crack length. A more detailed discussion of the energy release rate is given in section 3. Using the values of K_G and v_{\min} for normalization Eq. (28a) reduces to the following non-dimensional form

$$K/K_G = 0.845[(v/v_{\min})^{1/12} + (v/v_{\min})^{-1/12}] \quad (30)$$

Figure 7 shows the curve of the K/K_G vs v/v_{\min} on a log-log scale. It should be noted here that for $v < v_{\min}$ Eq. (30) predicts a decreasing v with an increasing K . We contend that this configuration is physically inadmissible since the predicted crack thickness $2w$ from Eq. (3) is large enough for $v < v_{\min}$ to render the model's basic assumption of long thin shape invalid. Further, the time-dependent analysis of Chuang et al. [4], indicates that the crack growth mode operates only at higher velocities. In the region of slow growth rates, the cavity is in quasi-equilibrium shape and consequently the low velocity portion of the curve is not valid.

It has been conventional to express the v - K curves in the form of $v = \text{const} \cdot K^n$ so that straight lines can be drawn on a log-log paper. In

an attempt to plot Eq. (30) in compliance with this form, we found that n is not a constant; its values range between 12 and ∞ depending upon the ratio of u/u_{\min} :

$u/u_{\min} = 1$	10	10^2	10^3	10^4	10^5	10^6	10^7	10^8	∞
$n = \infty$	63	33	23	19	16	15	14	13	12

as can be seen in figure (7). A fuller discussion of this plot as well as a comparison with experimental data are given in section 4.

3. The energy release rate in crack growth

It is well recognized that during crack propagation a portion of the energy is trapped inside the body which is not recoverable. This released energy due to increment in crack length provides a driving "force" for crack extension. The energy release rate \mathcal{G} , as a basic definition is therefore the decrease of the total potential energy P in the system due to infinitesimal increment of crack length da , i.e., $\mathcal{G} \equiv -dP/da$. Further, since $P \equiv Fe - W$, \mathcal{G} can be expressed in terms of the steady state crack tip velocity u as follows*

$$\mathcal{G} \equiv (\dot{W} - \dot{F}_e)/u \quad (31a)$$

where W and F_e are the mechanical work done by the external loads and the total strain energy stored in the interior of the body. The dot stands for the total derivative with respect to time. (e.g., $v = \dot{a}$)

The Griffith crack extension model is well known and assumes that all energy loss goes to the creation of new crack surfaces, no other plastic energy dissipation occurs. Thus, if F and F_s denote total and surface free energy of the body, respectively, then $\dot{F} = \dot{F}_e + \dot{F}_s$ and

*In transient state crack growth, \mathcal{G} is not definite since it depends on the surrounding stress and displacement fields which are changing continuously. The reader is referred to [12] for more detailed discussion.

energy balance requires that $\dot{W} = \dot{F} = \dot{F}_e + (2\gamma_s - \gamma_b)u$ so that

$$\mathcal{E}_{\text{Griffith}} = \dot{F}_s / u = 2\gamma_s - \gamma_b \quad (31-1)$$

This $\mathcal{E}_{\text{Griffith}}$ represents the absolute minimum energy consumption required for growing a crack. Any loading with a \mathcal{E} level below $\mathcal{E}_{\text{Griffith}}$ will not cause a crack to propagate and furthermore, at least in theory, healing ($u < 0$) would take place.

In contrast to the Griffith model, it is perhaps interesting to evaluate the energy release rate for our diffusive crack growth model. Since diffusion is an irreversible process leading to crack growth and since the grains are assumed to behave elastically, no energy loss occurs in the interior of the grains during crack growth. The unrecoverable energy involves only that associated with the surface and grain-boundary diffusional processes in addition to that which has to be spent on creation of the new crack surfaces. Accordingly, two extra terms associated with diffusion have to be added to the energy balance equation for the present model*. Thus,

$$\dot{W} = (\dot{F}_e + \dot{F}_s) + \dot{Q}_s + \dot{Q}_b$$

giving

$$\mathcal{E} = (\dot{F}_s / u) + (\dot{Q}_s / u) + (\dot{Q}_b / u) \quad (31b)$$

where \dot{Q}_s and \dot{Q}_b are the energy dissipation rates for surface and grain-boundary diffusion processes. These two quantities are in direct proportion to

$\int \underline{j} \cdot (-\nabla \mu) ds$ since $(-\nabla \mu)$ represents the chemical force exerts on an atom and $\underline{j} \cdot (-\nabla \mu) ds$ is therefore the total energy used to move atoms across ds per unit time at the location of our interest. In terms of non-equilibrium thermo-

*The kinetic energy is very small as compared to say work done by grain boundary normal stress on opening the crack tip, hence will be neglected in the subsequent discussions. For example, even at high u ($= 1 \mu\text{m/s}$) for sialon at 1400°C , the kinetic energy is $\approx 10^{-14}$ J/mol and the work done by σ_{tip} on opening δ_{tip} at the crack tip is ≈ 1 J per meter of crack front.

dynamics these terms represent local entropy production by irreversible diffusion flow at the free surfaces and interface. Equation (31b) agrees with the results obtained by Rice and Chuang [12] based on a detailed consideration of energy variations in cavity growth. (Cf. Eq. (16) of Ref. 12.) It is also in complete accord with the elaborations made by Speight et al. [6].

To evaluate \dot{Q}_s , we recall from Eqs. (1) and (4) that both J_s and μ_s decay exponentially along the crack surface from the tip. Thus, by noting that there are two crack surfaces we have from Eqs. (1), (5), and (6)

$$\begin{aligned} \dot{Q}_s &= 2 \int_{\Gamma_s} J_s (-\partial \mu_s / \partial s) ds \\ &= \gamma_s \Omega \kappa_{tip} (J_s)_{tip} \\ &= (2\gamma_s - \gamma_b) u \end{aligned} \tag{32}$$

Surprisingly, we find that the surface diffusion component of \mathcal{S} is identical to the Griffith energy, $2\gamma_s - \gamma_b$ and is independent of the crack tip velocity, u .

To proceed with evaluation of \dot{Q}_b we found it useful to introduce a new parameter, J --a path-independent integral discovered by Rice [13]:

$$J = \int_{\Gamma} w dx_2 - \vec{T} \cdot \partial \mu / \partial x_1 ds \tag{33a}$$

Here Γ is an arbitrary integration path surrounding the crack tip starting from the lower crack surface and proceeding in a counter-clockwise fashion to the upper one; w is the local strain energy density; and \vec{T} and μ are the traction and displacement vectors acting on the path. In our model,

it is possible to evaluate J by choosing a special path as indicated in figure 1 starting from the point immediately below the tip following the lower boundary surface, Γ^- , to infinity, crossing the boundary there and returning to the point immediately above the tip by following the upper boundary surface, Γ^+ . In this way, it is evident that only the upper and lower path integration along g.b., Γ^+ and Γ^- contribute to J since along the vertical path at $x = +\infty$, the values of w , \underline{u} and \underline{u} have decayed to zero.

Thus

$$\begin{aligned}
 J &= - \int_0^{\infty} \sigma \partial(u^+ - u^-) / \partial x dx \\
 &= - \int_0^{\infty} \sigma (\partial \delta / \partial x) dx
 \end{aligned}
 \tag{33b}$$

Here the first term of J in Eq. (33a) involving w is dropped due to $dx_2 = 0$ for both upper and lower paths, and $u^+(x)$ and $u^-(x)$ denote the displacements in the direction of x_2 at the upper and lower surfaces of the grain boundary, respectively, such that $\delta(x) = U^+(x) - U^-(x)$. It is interesting to note, in the context of evaluating J , that by reducing both Γ^+ and Γ^- as shown in figure 1 to a finite length, the situation of the well-known Dugdale model is obtained. Thus in a sense the Dugdale model which has a finite cohesive zone ahead of the stationary crack tip can be regarded as a special case of the present crack growth model in which the "cohesive forces" cover the whole length of the grain boundary. With the help of Eq. (33b) we proceed to evaluate \dot{Q}_b in the following way

$$\begin{aligned}
\dot{Q}_b &= \int_0^{\infty} J_b (-\partial \mu_b / \partial x) dx \\
&= \int_0^{\infty} J_b \Omega (\partial \sigma / \partial x) dx \\
&= v \int_0^{\infty} \delta (\partial \sigma / \partial x) dx \\
&= -\delta_{\text{tip}} \sigma_{\text{tip}} v - v \int_0^{\infty} \sigma (\partial \delta / \partial x) dx \\
&= -2w \kappa_{\text{tip}} \gamma_s v + vJ \\
&= [-2(2\gamma_s - \gamma_b) + J]v \tag{34}
\end{aligned}$$

Here, the second equality follows from Eq. (7), the third from Eq. (12a), the fourth is obtained by integration by parts, the fifth by Eqs. (33b), (12b), and (10), and the final equality by Eqs. (3) and (6).

The final expression of \mathcal{E} results in the following simple form after combining Eqs. (31-1), (32), and (34) into Eq. (31b):

$$\mathcal{E} = J \tag{35}$$

This equation shows that J is indeed the correct energy release rate for our diffusive crack growth model as is true in the theory of elastic fracture mechanics.

Alternatively, it is straightforward to evaluate \mathcal{E} from the standpoint of mechanics. From the theory of linear elasticity, the rate of change of strain energy inside the body due to material removal from the

crack surfaces and addition to the grain boundary [14-16] is

$$\dot{F}_e = 2 \int_{\Gamma_s} w \dot{\delta} ds + \int_{\Gamma_b} w \dot{\delta} ds + \dot{W} - \int_{\Gamma_b} \sigma \dot{\delta} ds$$

However, the first two integrals involving w are negligible due to low w since the stress levels developed even in the vicinity of the crack tip are low (see figure 6). Thus

$$\begin{aligned} \mathcal{E} &\equiv (\dot{W} - \dot{F}_e)/v \\ &= (1/v) \int_0^{\infty} \sigma \dot{\delta} ds \\ &= (1/v) \int_0^{\infty} \sigma [-v(\partial\delta/\partial x)] dx \\ &= J \end{aligned}$$

where the steady state condition $\dot{\delta} = -v \partial\delta/\partial x$ has been used. Hence we see that the two independent approaches for evaluating \mathcal{E} , one based on consideration of diffusive energy dissipation; another derived from theory of elasticity, both lead to the same conclusion that $\mathcal{E} = J$ is indeed the correct energy release rate.

In what follows we attempt to prove that

$$\mathcal{E} = J = (1-\nu^2)K^2/E \quad (36)$$

in the present crack growth model as is true in the case of elastic fracture mechanics.

Using Eq. (13) to eliminate $\delta(x)$ and performing integration by parts, allow Eq. (36) to be transformed into the following form

$$\hat{K} = (2/\sqrt{\pi}) \left[\alpha + \int_0^{\infty} (\hat{\sigma}')^2 d\hat{x} \right]^{1/2} \quad (37a)$$

where \hat{K} and $\hat{\sigma}'$ are non-dimensional versions of K and σ' defined as follows

$$\hat{K} = K/(\sigma_{\text{tip}} \sqrt{L}) \quad (37b)$$

$$\hat{\sigma}' = L\sigma'/\sigma_{\text{tip}} \quad (37c)$$

Our task is to provide the proof of the equality shown in Eq. (37a)

regardless of the value of α and, thereby, establish the identity:

$\mathcal{E} = (1-\nu^2)K^2/E$. To do so, we first recall that $\hat{\sigma}' = \hat{\sigma}'_0 + \alpha\Delta\hat{\sigma}'$ from Eq. (26)

and $K = \sqrt{2\pi} (0.24\alpha + 0.30)$ from Eq. (A15). Accordingly, the following

three equalities have to be simultaneously satisfied if Eq. (37a) holds for

any value of α :

$$\int_0^{\infty} (\hat{\sigma}'_0)^2 d\hat{x} = \frac{1}{2} (\pi \times 0.3)^2 \cong 0.44413 \quad (38a)$$

$$\int_0^{\infty} (\Delta\hat{\sigma}')^2 d\hat{x} = \frac{1}{2} (\pi \times 0.24)^2 \cong 0.28424 \quad (38b)$$

$$\int_0^{\infty} \hat{\sigma}'_0 \cdot \Delta\hat{\sigma}' d\hat{x} = \frac{1}{2} (\pi^2 \times 0.3 \times 0.24 - 1) \cong -0.14469 \quad (38c)$$

To prove these identities, Eqs. (38a-c), we performed direct numerical integrations on $(\hat{\sigma}'_0)^2$, $(\Delta\hat{\sigma}')^2$, and $(\hat{\sigma}'_0 \cdot \Delta\hat{\sigma}')$ as given by solutions obtained in section 2.4 (see figure 4). Table 1 shows the numerical values obtained by these solutions and comparisons to the values given by Eqs. (38a-c). It is seen that the difference between the two columns is less than five percent error margin. Hence it can be concluded that in the present model $(1-\nu^2)K^2/E$ is indeed the correct energy release rate which is consumed in creation of

new crack surfaces and in completion of surface and grain-boundary diffusion processes. Alternatively in mechanics term, \mathcal{G} or J has been shown to be directly related to the work done by the normal stress in opening up the grain boundary as indicated by expression of J in Eq. (33b).

Equation (36) shows that the total energy release rate is dependent on the crack velocity. From this equation it is possible to compute \mathcal{G} for the present model. At $v = v_{\min}$, for example, we find $\mathcal{G} = 2.85 \mathcal{G}_{\text{Griffith}}$ from Eqs. (29b) and (36), far exceeding $1.0 \mathcal{G}_{\text{Griffith}}$, the absolute minimum level*. This is expected from the energy balance considerations. The total amount of energy loss can be further split into the following items: $1.0 \mathcal{G}_{\text{Griffith}}$ is attributed to the creation of new surfaces as in the case of Griffith cracks; the identical amount of energy is spent on surface diffusion; and the remaining $0.85 \mathcal{G}_{\text{Griffith}}$ is consumed in grain boundary diffusion. However, as v increases due to a higher level of applied stress, the former two items remain fixed and the increased energy loss goes solely to the last term, since both \dot{F}_s/v and \dot{Q}_s/v are not function of v whereas \dot{Q}_b/v is (see Eqs. (31-1), (32), (34)).

4. Discussion

We have presented a steady state solution relating the applied stress intensity to the crack tip velocity for the grain boundary crack growth model proposed here, assuming that the crack growth is controlled by stress-assisted surface and grain-boundary self-diffusion and the adjoining grains behave elastically. This solution identifies K , the crack tip stress intensity factor defined in the absence of diffusion, as the major parameter in controlling the driving force of the creep crack growth although the true

*Other diffusive crack growth models considered in Ref. 10 all indicate that $\mathcal{G} > \mathcal{G}_{\text{Griffith}}$. For example, at $v = v_{\min}$, $\mathcal{G} = \mathcal{G}_{\min} = 4.5 \mathcal{G}_{\text{Griffith}}$ for a spring model and $\mathcal{G}_{\min} = 6.45 \mathcal{G}_{\text{Griffith}}$ for a double cantilever beam model.

stress field no longer exhibits stress singularity at the moving crack tip (Cf., figure 6). Further, the solution was obtained from a rigorous analysis of the coupled effects of diffusion and elastic deformability in which diffusion equations and conservation of mass are satisfied at both crack walls and along the grain boundary including the crack tip, and the associated stress and displacement fields not only satisfy the equilibrium and compatibility requirements at any point inside the body but also yield to the appropriate boundary conditions at the crack plane and the outer boundaries where the external loads are prescribed.

A similar crack growth model based on the assumptions set out in section 2.1 was proposed by Vitek [5]. However, as discussed earlier, two extra assumptions about the crack shape were made in that model. First, a point called A was introduced somewhere on the crack surface across which the slopes of the crack shape profile are discontinuous. This leads to an undefined κ (and hence μ_s) at A, making Eq. (2) governing surface diffusion inapplicable in the neighborhood of A. Physically, surface "faceting" can occur due to the anisotropic nature of crystallographic orientations. However, under the assumption of surface isotropy on a macroscopic scale implicitly invoked in this work and also by Vitek, this configuration is not in thermodynamic equilibrium. As a consequence, the surface facet or discontinuous slope, would be "smoothed" out by the long-term diffusion process. Second, the crack thickness, $2w$, given by Eq. (3) based on a detailed analysis of the crack shape was not adopted in that model, instead an arbitrary constant thickness, independent of v , was assumed. It is difficult to justify using a particular thickness due to its arbitrary nature although some identifiable physical parameters

such as crack opening displacement can be used as suggested by Vitek. His paper also criticises Eq. (3) because that equation not only predicts decreasing crack thickness with increasing growth rate, but also because it predicts physically unattainable velocities for α -iron at 550 °C. In response to this criticism, we emphasize that Eq. (3) does indeed predict a constant crack thickness at steady state in which v is stationary. It is when the crack growth rate changes from one steady state to another, perhaps due to a change in load or temperature, does Eq. (3) predict a decreasing $2w$ with increasing v . A discussion of the transient behavior is outside the scope of the present paper although a brief remark is in order here. According to a recent study [17] of cavity morphology, resulting from crack growth in transient state, it was shown that when the applied stress is high as compared to the sintering stress, a "nose" region develops ahead of the cavity apex and the direction of the surface flux near the central portion is actually reversed. This causes the crack thickness to decrease in close accord with Eq. (3). A scanning electron micrograph of silver showing nose regions on grain boundary cavities was also provided as evidence to support that analysis. These interesting results support the validity of Eq. (3). The high crack velocities calculated for α -Fe using Eq. (3) may indicate that some other mechanisms, not considered in our model, are controlling crack growth.

Because of the two extra conditions (a discontinuous slope and a constant crack thickness), Vitek's model suffers the following consequences: (1) the crack tip conditions regarding μ_s and J_s are not properly formulated, as we have done in section 2.2, with the result that the normal stress at the crack tip remains constant independent of v (and hence independent of the

applied stress); and (2) mass conservation at the crack tip, Eq. (9b), dictating σ'_{tip} could not be used. Instead the physical requirement that $\sigma(x)$ far away from the tip approach asymptotically to the stress field induced by the applied stress in the absence of diffusion was imposed (see Eq. (14) of Ref. 5). It is noted that in our model this physical behavior was obtained directly from the solutions shown in figure 6. It remains to be proved that the solutions based on Vitek's boundary conditions will automatically make Eq. (9b) valid.

Speight et al. [6] have proposed a crack growth model similar to what has been presented here. In contrast to our model (see fig. 5) as well as Vitek's, the grain boundary displacement distribution, $\delta(x)$, was not pursued in their analysis. Instead, a parabolic function of $\delta(x)$ was imposed (see Eq. (1) of Ref 6) such that δ and δ' vanish at a short distance ($x = b$) from the crack tip. A consideration of the energy release rate associated with crack growth was also incorporated in their formulation. We have shown in section 3 that J or $(1-\nu^2)K^2/E$ is the correct energy release rate of which, at $\nu = \nu_{min}$, thirty-five percent goes to creation of new crack surfaces, another thirty-five percent is spent in the process of surface diffusion, and the remaining thirty percent is consumed by grain-boundary diffusion. As ν increases, the former two terms remain fixed and the excess energy is dissipated in the grain boundary as a form of mechanical work done by the boundary normal stresses. In contrast to the present analysis, Speight et al. contend that the total plastic work of $2\omega w$ by the applied stress σ_{∞} is the total energy released during the growth period, i.e., $\mathcal{E} = 2\sigma_{\infty} w$. This contention implies that the adjoining grains behave rigidly so that the opening displacement, $\delta(x) = 2w$, are uniformly distributed along the grain boundary. This is in direct contradiction

to their Eq. (1). Further, it has been shown in Ref. 12 that this term $2\sigma_{\infty}\omega$, appears to be minor in the total energy release expression. As a result of these assertions, the peak stress is predicted to have a value linearly dependent on σ_{∞} at a fixed point $x = b$, $\sigma(b) = \frac{5}{3} \sigma_{\infty}$. In contrast our solutions show how the values of the peak stress varies depending on the values of α and L which in turn are functions of ν (see figure 6). Finally, their model is claimed to be applicable to a relatively short crack but this is not in agreement with the conclusions obtained by Chuang et al. [4] based on a time-dependent study. There it was shown that, when the cavity size is small, presumably in the early stage, the cavity maintains a quasi-equilibrium shape and as the creep test continues, the cavity gradually becomes long and crack-like as its growth rate increases. The present, long crack model, which includes the prediction of fast growth, fits well in this time-dependent analysis.

Attempts have been made to evaluate the theoretical predictions for K_{min} , ν_{min} , and K versus ν curve in the case of pure Cu, Ni, α Fe, γ Fe, Zn, and Ag [10]. It was found that of the six metals, only Ni and Cu yield physically tenable values for ν_{min} . It is fair to say that the materials property data employed for this evaluation involved some degree of uncertainty. Nevertheless, it is likely that for pure metals some mechanisms not considered in our paper (particularly some dislocation processes) are in operation during creep. As pointed out before, the theory was developed for strong brittle materials. Thus it is worthwhile to compare our theory with the data on ceramics. Recently, Lewis and Karunaratne [7] have performed creep tests on Si-Al-O-N ceramics at 1400 °C. In their tests three different techniques were used to measure crack growth rate depending on the range of crack velocities.

In this way they were able to produce reliable, continuous curves on a K vs V plot. It was found in the ceramic specimen C that the sub-critical crack growth occurs via the advance of a single crack along the grain boundaries. The growth behavior can be well described by [7]

$$K = 3.5 \times 10^6 \nu^{1/12} + 7.4 \times 10^4 \nu^{-1/12} \quad (39)$$

where K is in units of $\text{Pa}\cdot\text{m}^{1/2}$; and ν in m/s . This experimental result is identical to what the model predicts in equation (28a) where $A = 3.5 \text{ MN}\cdot\text{m}^{-19/12}\text{S}^{1/12}$ and $B = 74 \text{ KN}\cdot\text{m}^{-17/12}\cdot\text{S}^{-1/12}$. The coefficients of Eq. (39) were computed from the data listed in table 2.

The creep test data are also plotted against our theoretical curve in figure 7. It is seen that the majority of the data points (except the lowest three data points) fall along the curve, close enough to lead us to conclude that the theory successfully predicts not only the functional dependence of crack velocity on applied stress intensity factor, but also the absolute magnitude of crack tip velocity. The deviation in functional dependence in the low velocity range may indicate the flaw shapes no longer preserve the crack-like shapes.

All relevant parameters for the creep tests are also calculated in table 3. Examination across the board shows that the values of most parameters do fall in physically reasonable ranges except $2w$ which seems to be about one order too low. At those data points for which $\nu/\nu_{\min} \approx 10^3 \sim 10^4$, the crack thickness $2w$ reduces to the same order as the atomic spacing (0.2 nm). It is possible that both surface and grain boundary diffusivities are one order lower. If such is the case, then all parameters do fall in the appropriate values. Owing to the scarcity

of the creep crack growth data it is clear that more measurements are needed, but qualitatively our theory seems to be well supported by creep tests on sialons.

5. Summary and Concluding Remarks

From what we have presented on the present crack growth model, the following concluding remarks may be given.

5.1 If steady state interfacial crack growth is controlled by coupled surface and grain-boundary diffusion and if the adjoining grains behave elastically then the crack tip stress intensity factor K in the absence of diffusion is identified as the correct parameter driving creep crack growth. The functional relationship between K and ν is found to be $K/K_G = 0.865 \times [(\nu/\nu_{\min})^{1/12} + (\nu/\nu_{\min})^{-1/12}]$. This equation predicts that a threshold K equal to $1.69 K_G$ exists, where K_G is the critical K for Griffith cracks, below which no crack growth can take place. In terms of $\nu = \text{const. } K^n$ on a log-log scale, this equation predicts the slope n varying between 12 and infinity depending on the value of ν . The features of the sub-critical crack growth behavior so predicted are also consistent with that obtained from a time-dependent analysis [4].

5.2 The path-independent integral J or the plane strain fracture mechanics energy release rate $(1-\nu^2)K^2/E$ is shown to be the correct energy release rate associated with creep crack growth. This energy is dissipated in the creation of new crack surfaces, as well as in the completion of surface and grain boundary diffusional processes. However, it was found that the energy loss is in the form of work done by grain boundary normal stresses due to deposition of atoms along the grain interface rather than the release of strain energy in the near-tip region as is the case in conventional fracture mechanics.

5.3 Excellent agreement is obtained when the predictions are compared with a set of test data on creep crack growth for Si-Al-O-N at 1400 °C. It is concluded, at least qualitatively, that under appropriate conditions, sub-critical creep crack growth behavior of ceramics closely follows what is predicted by the present theory.

Acknowledgments

A portion of this study (sections 2 and 6) was based on a part of the author's Ph.D. thesis and was supported by the U. S. Department of Energy (formerly U. S. Atomic Energy Commission) under contract EY-76-S-02-3084-A003 with Brown University. The remaining portion of the work was supported by the Department under interagency agreement DE-AI05-800R20679 between DOE and the National Bureau of Standards.

The author is grateful to his thesis adviser, Professor James R. Rice for his effective direction, and to his colleagues, Dr. Richard J. Fields and Dr. Edwin R. Fuller, Jr., for providing the computer plot of figure 7 and for proofreading the manuscript.

Appendix

Numerical Solution Scheme for integral Equation (24)

In this appendix we present a solution scheme to the following 1D Fredholm-type integral equation for the unknown function $\psi(x)$ as appeared in the text, equation (24):

$$\psi(x) = f(x) + \int_0^{\infty} K(x,t) \psi(t) dt \quad (A1)$$

wherein $K(x,t)$ is the kernel and $f(x)$ a given function:

$$K(x,t) = (x-t) \ln|x-t| - (x-t) \quad (A2)$$

$$f(x) = \ln x + \alpha x (\ln x - 1) \quad (A3)$$

The unknown function $\psi(x)$ has been defined in the text as the second derivative of normal stress with respect to x along the grain boundary ($0 \leq x < \infty$) and is presumed to satisfy the following conditions:

(1) $\psi(x)$ is integrable;

(2) $\lim_{x \rightarrow \infty} x^2 \psi(x) = 0$

These two mathematical assumptions are based on the physical arguments that a unique stress solution does exist and its asymptotic behavior as $x \rightarrow \infty$, as depicted by linear fracture mechanics theory makes conditions (1) and (2) valid.

Since closed form solutions exist only for a limited class of integral equations, we shall pursue the solution of equation (A1) numerically with the aid of digital computers. To solve (A1) numerically, we employ the standard method of replacing the integral equation with a system of coupled

linear algebraic equations, assuming the integral $\int_0^{\infty} K\psi dt$ can be represented

by a finite sum. In trying to do so, we encounter two difficulties. First as pointed out in the text, $\psi(x)$ has a logarithmic singularity at $x = 0$ which makes the direct numerical integration from $x = 0$ impossible; secondly, the upper limit extends to infinity which also apparently cannot be reached. To avoid these two areas of difficulty, it is therefore necessary to introduce two cut-off points, say $x_1 \rightarrow 0$ and $x_n \rightarrow \infty$ so that integration over $[x_1, x_n]$ can give an approximate value of the integral. This means that if we write

$$\int_0^{\infty} K(x,t)\psi(t)dt = \int_{x_1}^{x_n} K(x,t)\psi(t)dt + \int_0^{x_1} K\psi dt + \int_{x_n}^{\infty} K\psi dt \quad (A4)$$

then the second and third terms on the right hand side are small as compared to the first term. However, in order to increase the accuracy of the results, it is desirable to evaluate the second and third terms as well*. The asymptotic behaviors of ψ allow us to write

$$\int_0^{x_1} K\psi dt \sim \int_0^{x_1} K(x,t)\ln t dt, \quad x \geq x_1$$

and

$$\int_{x_n}^{\infty} K\psi dt \sim \int_{x_n}^{\infty} K(x,t)t^{-5/2} dt, \quad x \leq x_n$$

*The solution of the system without addition of these two terms has also been pursued which showed satisfactory results. However, by including these two terms the results showed faster convergence and therefore improve the accuracy of the solutions.

Carrying out the integration analytically, one obtains

$$\begin{aligned}
 L(x, x_1) &\equiv \int_0^{x_1} K(x, t) \ln t \, dt \\
 &= (x-x_1)[(x+x_1 \ln x_1) \ln(x-x_1) - (x_1 \ln x_1 - x_1)] \\
 &+ x^2 (\ln x + \frac{7}{4}) - (x-x_1)(3x+x_1)/2 \\
 &+ \frac{1}{4} [2 \ln x - 2(\frac{x_1}{x}) - (\frac{x_1}{x})^2] x_1^2 \ln x_1 \\
 &+ (x^2 - \frac{x_1^2}{2}) \ln x_1 \sum_{n=3}^{\infty} \frac{(\frac{x_1}{x})^n}{n} - x^2 \sum_{n=3}^{\infty} \frac{(\frac{x_1}{x})^n}{n^2}
 \end{aligned}$$

for $x \geq x_1$ (A5.1)

$$\begin{aligned}
 R(x, x_n) &\equiv \int_{x_n}^{\infty} K(x, t) t^{-5/2} \, dt \\
 &= \frac{4}{3} (x^{-1/2} - x_n^{-1/2}) \ln(x_n - x) - \frac{8}{3} x^{-1/2} \ln(\sqrt{x} + \sqrt{x_n}) \\
 &- \frac{2}{3} x_n^{-3/2} [(x_n - x) \ln(x_n - x) - (x_n - x)];
 \end{aligned}$$

for $x \leq x_n$ (A5.2)

We observe that both $L(x, x_1)$ and $R(x, x_n)$ are bounded even at $x = x_1$ and $x = x_n$. The interval $[x_1, x_n]$ is divided into $(n-1)$ subintervals with n discrete points x_1, x_2, \dots, x_n excluding the point $x = 0$. Denoting $\psi_i = \psi(x_i)$, our objective is then to find the n unknown values of ψ_i , $i = 1$ to n , by assuming that any two adjacent points (x_i and x_{i+1}) are sufficiently close so that $\psi(x)$ can be assumed to vary linearly between ψ_i and ψ_{i+1} . Thus

$$\psi(x) \cong \left(\frac{\psi_{i+1} - \psi_i}{x_{i+1} - x_i} \right) x + \left(\frac{x_{i+1} \psi_i - x_i \psi_{i+1}}{x_{i+1} - x_i} \right)$$

$$\text{for } x_i \leq x \leq x_{i+1} \quad (A6)$$

To proceed, we observe that the first term on the right hand side of (A4) can be decomposed into the following sum:

$$\int_{x_1}^{x_n} K \psi dt = \sum_{i=1}^{n-1} \int_{x_i}^{x_{i+1}} K(x, t) \psi(t) dt \quad (A7)$$

Denoting

$$F(x, x_i, x_{i+1}) \equiv \int_{x_i}^{x_{i+1}} t K(x, t) dt \quad (A8)$$

and

$$G(x, x_i, x_{i+1}) \equiv \int_{x_i}^{x_{i+1}} K(x, t) dt \quad (A9)$$

and substituting ψ of (A6) into (A7), the integral equation (A1) finally reduced to the following simultaneous equations:

$$([K] - [I]) \{\psi\} = -\{f\}. \quad (A10)$$

where $[K]$ is a $n \times n$ matrix, $[I]$ is a unity matrix and $\{f\}$ is a vector with typical element $f_j = f(x_j)$. The typical element of $[K]$ can be written as follows for $j = 1$ to n :

$$K_{j1} = \frac{x_2 G(x_j, x_1, x_2) - F(x_j, x_1, x_2)}{x_2 - x_1} + \frac{L(x_j, x_1)}{\ln x_1}$$

$$K_{ji} = \frac{x_{i+1} G(x_j, x_i, x_{i+1}) - F(x_j, x_i, x_{i+1})}{x_{i+1} - x_i} - \frac{x_{i-1} G(x_j, x_{i-1}, x_i) - F(x_j, x_{i-1}, x_i)}{x_i - x_{i-1}}$$

(i = 2 to n-1)

$$K_{jn} = \frac{F(x_j, x_{n-1}, x_n) - x_{n-1} G(x_j, x_{n-1}, x_n)}{x_n - x_{n-1}} + x_n^{5/2} R(x_j, x_n)$$

where L, R, F, G are functions defined in (A5.1), (A5.2), (A8), and (A9) respectively.

A computer FORTRAN program was developed to solve $\{\psi\}$ in equation (A10)

in which the following parameters were chosen: $n = 200$, $x_1 = 0.01$,

$x_n = 58.2$ and

Integration range: [0.01, 1.2] [1.2, 2.2] [2.2, 8.2] [8.2, 18.2] [18.2, 58.2]

Interval Δx : 0.01 0.05 0.2 1.0 2.0

Thus a non-uniform distribution of x_j results, having a more dense distribution near the origin where the behavior of ψ is of major interest.

To test the validity of the FORTRAN program, an integral equation of the form (A1), with the same kernel as given in (A3) was chosen where $f(x)$ is given by

$$f(x) = (x+a)^{-5/2} + \frac{4}{3} (x+a)^{-1/2} \ln \left[\frac{(x+a)^{1/2+a^{1/2}}}{(x+a)^{1/2-a^{1/2}}} \right] + \frac{4}{3} a^{-1/2} \ln x$$

$$-\frac{2}{3} a^{-3/2} (x \ln x - x)$$

(A11)

and its closed form solution is known as

$$\psi(x) = (x + a)^{-5/2} \quad (A12)$$

Equation (A11) was input to the program with $a = 1$ and the solution given by the output of the program was then compared with the analytical curve of (A12) which shows a negligible difference between the two solutions. The reliability of this computer program was hence confirmed.

Using this program with the input of f given by (A2), the solutions of equation (A1) for ψ were obtained first for $\alpha = 0$ and 20, respectively. The results show that values of $x^{5/2}\psi(x)$ do attain an approximately constant value of a distance far away from the origin, say for $x \geq 8.0$, and as remarked above, this should be set equal to $\frac{3}{4} \frac{K}{\sqrt{2\pi}}$. The correctness of these solutions can be further verified from the initial conditions on stress at $x = 0$ which take the following form:

$$\int_0^{\infty} \psi(x) dx = -\alpha \quad (A13)$$

$$\int_0^{\infty} x\psi(x) dx = 1 \quad (A14)$$

The numerical integrations of the left-hand sides of equations (A13) and (A14) were performed, using Simpson's rule which yield the following results:

$$\int_0^{\infty} x(\psi)dx = -0.17651^* \text{ for } \alpha = 0$$

$$= -21.71512^* \text{ for } \alpha = 20$$

$$\int_0^{\infty} x\psi(x)dx = 0.99551^* \text{ for } \alpha = 0$$

$$= 0.97582^* \text{ for } \alpha = 20$$

From these numerical results, it can be said that the convergence of the solution is fairly rapid and the accuracy of the solution is within five percent error range.

The structure of the integral equation (A1) indicates that the non-dimensionalized stress intensity factor K should be linearly dependent on α . Indeed, this is verified by the solutions of ψ for $\alpha = 1.0, 1.5, 2.0, 2.5$. A plot of $\hat{K}/\sqrt{2\pi}$ vs α shows that

$$\hat{K}/\sqrt{2\pi} = 0.24 \alpha + 0.30 \quad (\text{A15})$$

as given by equation (27) in the text.

The stress distribution $\hat{\sigma}(x)$ can be obtained by integration of ψ twice. This was done on the two solutions of ψ corresponding to $\alpha = 0$ and $\alpha = 20$. The results show that at large distances from the origin, $x^{1/2}\hat{\sigma}(x)$ does not attain a stationary value, instead it either rises or falls linearly. This phenomenon was not surprising because any disturbance caused by errors unavoidably induced in $\hat{\sigma}(x)$ by numerical integration as $a + bx$ contributes nothing to ψ . Therefore, a correction should be made over the whole range

of x for $\hat{\sigma}$ according to the guideline that $\sqrt{x}\hat{\sigma}$ must approach $\hat{K}/\sqrt{2\pi}$ for $x \geq x_n$, for example. Figure 6 shows the curves of $\hat{\sigma}(x)$ vs x for $\alpha = 0, 1, 5, 10,$ and 20 , respectively, after the corrections have been made.

*Values include analytical integration over $[x_n, \infty)$.

References

1. D. Hull and D. E. Rimmer, "The Growth of Grain-boundary Voids Under Stress," *Philos. Mag.*, 4 [42], 673-687 (1959).
2. R. Raj and M. F. Ashby, "Intergranular Fracture at Elevated Temperature," *Acta Metall.*, 23 [6], 653-666 (1975).
3. T.-J. Chuang and J. R. Rice, "The Shape of Intergranular Creep Cracks Growing by Surface Diffusion," *ibid.*, 21 [12], 1625-1628 (1973).
4. T.-J. Chuang, K. I. Kagawa, J. R. Rice, and L. B. Sills, "Overview No. 2: Non-equilibrium Models for Diffusive Cavitation of Grain Interfaces," *ibid.*, 27 [2], 265-284 (1979).
5. V. Vitek, "A Theory of Diffusion Controlled Intergranular Creep Crack Growth," *ibid.*, 26 [9], 1345-1356 (1978).
6. M. V. Speight, W. B. Beere, and G. Roberts, "Growth of Intergranular Cracks by Diffusion," *Mater. Sci. Eng.*, 36 [2], 155-163 (1978).
7. M. H. Lewis and B. S. B. Karunaratne, "Determination of High Temperature K_I -V Data for Si-Al-O-N Ceramics," submitted to ASTM STP publication.
8. B. R. Lawn, B. J. Hockey, and S. M. Wiederhorn, "Atomically Sharp Cracks in Brittle Solids: An Electron Microscopy Study," *J. Mater. Sci.*, 15 [], 1207-1223 (1980).
9. A. Needleman and J. R. Rice, "Overview No. 9: Plastic Creep Flow Effects in the Diffusive Cavitation of Grain Boundaries," *Acta Metall.*, 28 [10], 1315-1332 (1980).
10. T.-J. Chuang, "Models of Intergranular Creep Crack Growth by Coupled Crack Surface and Grain Boundary Diffusion," *Univ. Microfilms Int.* (Ann Arbor, Michigan) Order No. 76-15618, 95 pp.; *Diss. Abstr. Int. B*, 37 [1] 402 (1976).
11. R. N. Stevens and R. Dutton, "The Propagation of Griffith Cracks at High Temperatures by Mass Transport Processes," *Mater. Sci. Eng.*, 8 [4] 220-234 (1971).
12. J. R. Rice and T.-J. Chuang, "Energy Variations in Diffusive Cavity Growth," *J. Am. Ceram. Soc.*, 64 [1], 46-53 (1981).
13. J. R. Rice, "A Path Independent Integral and the Approximate Analysis of Strain Concentration by Notches and Cracks," *J. Appl. Mech.*, 35 [6] 379-386 (1968).
14. J. R. Rice and D. C. Drucker, "Energy Changes in Stressed Bodies Due to Void and Crack Growth," *Int. J. Fract. Mech.*, 3 [1] 19-27 (1967).

15. J. R. Rice; pp. 191-311 in Fracture, Vol. II. Edited by H. Liebowitz, Academic Press, New York, 1968.
16. J. D. Eshelby; pp. 77-115 in Inelastic Behavior of Solids, Edited by M. F. Kanninen, W. F. Adler, A. R. Rosenfield, and R. I. Jaffee, McGraw-Hill, New York, 1970.
17. G. M. Pharr and W. D. Nix, "A Numerical Study of Cavity Growth Controlled by Surface Diffusion," Acta Metall., 27 [10], 1615-1631 (1979).

Figure Captions

Figure 1 Geometry of the grain-boundary crack growth model. (x_1, x_2) is a cartesian coordinate system fixed in space, whereas (x, x_2) is moving with the crack tip at the velocity of v such that $x = x_1 - vt$.

Figure 2. Schematic sketches of configurations where the stress field of figure 2a containing a crack due to an edge dislocation can be computed from superposition of stress field produced by a dislocation in an external stress free body, figure 2b and that induced by the dislocational image forces applied at the crack site, figure 2c.

Figure 3. Numerical solutions of ψ vs \hat{x} for typical values of α .

Figure 4. Basic solutions of $\hat{\sigma}_0$ and $\Delta\hat{\sigma}$ and their first derivatives with \hat{x} from which any solution of $\hat{\sigma}$ or δ with a given α is obtainable from $\hat{\sigma} = \hat{\sigma}_0 + \alpha\Delta\hat{\sigma}$, or $\delta = (\hat{\sigma}'_0/\alpha) + \Delta\hat{\sigma}'$.

Figure 5. Typical solutions of δ vs \hat{x} for different values of α . Note that the curve for $\alpha = \infty$ crosses the $\delta = 0$ line at $\hat{x} = 0.9$.

Figure 6. Typical solutions of $\hat{\sigma}$ vs \hat{x} for several values of α . Stresses are seen to peak within the region of $0 < \hat{x} < 0.9$. For sake of comparison, stress distributions with and without diffusion are plotted for $\alpha = 20$.

Figure 7. Theoretical plot of normalized K vs v curve with correlated creep crack growth data for Si-Al-O-N at 1400 °C [7].

Table 1

Comparison of Numerical Values of Integrals Given by
Figure 4 and by Equations (38 a-c)

Integral	Numerical Integration Based on Figure 4 ¹	Value Given by Equations (38)	Percent Error
$\int_0^{\infty} (\hat{\sigma}'_0)^2 d\hat{x}$	0.43382	0.44413	2.32
$\int_0^{\infty} (\Delta\hat{\sigma}')^2 d\hat{x}$	0.28571	0.28424	0.52
$\int_0^{\infty} \hat{\sigma}'_0 \cdot \Delta\hat{\sigma}' d\hat{x}$	-0.13787	-0.14469	4.71

¹The method of numerical integration follows Simpson's rule, namely,

$$\int_{x_0}^{x_n} y(x) dx \approx \frac{\Delta x}{3} (y_0 + 4y_1 + 2y_2 + 4y_3 + \dots + y_n) \text{ where } y_i = y(x_i),$$

$i = 0, 1, \dots, n.$

Table 2

Summary of Material Property Data for Sialon at 1400 °C
 Used in Obtaining Equation (39)

Atomic volume, $\Omega(\text{m}^3)$	1.06×10^{-29}
Grain boundary diffusivity, $D_b \delta_b (\text{m}^3/\text{s})$	6×10^{-25}
Poisson's ratio, ν	0.27
Young's modulus, $E(\text{GNm}^{-2})$	300
Assumed surface diffusivity, $D_s (\text{m}^2\text{s}^{-1})$	2.5×10^{-18}
Assumed surface energy, $\gamma_s (\text{Jm}^{-2})$	0.75
Assumed grain boundary energy, $\gamma_b (\text{Jm}^{-2})$	0.375

Table 3

Calculated Values of Relevant Parameters for Creep
Crack Growth of Si-Al-O-N at 1400 °C

Parameter	Unit	Eq.No.	Value
K_G	MPa· \sqrt{m}	31	0.6
K_{min}	MPa· \sqrt{m}	30	1.0
v_{min}	nm s ⁻¹	29	0.09
$(L)_{umin}$	nm	19	990.0
$(\alpha)_{umin}$	--	23	1.26
$(\sigma_{tip})_{umin}$	MPa	10	717.0
$(2w)_{umin}$	nm	3	3.14

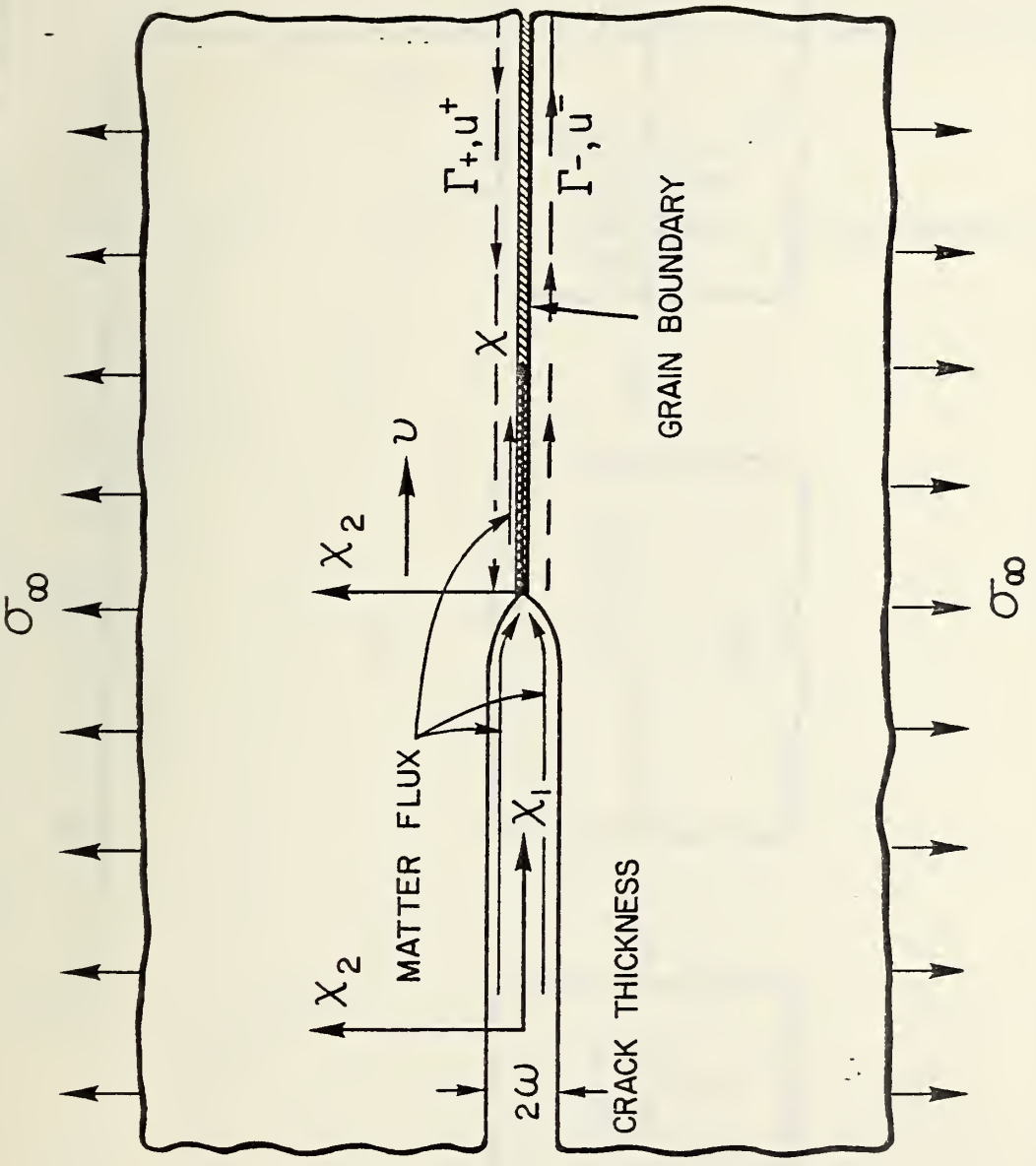


Fig 1

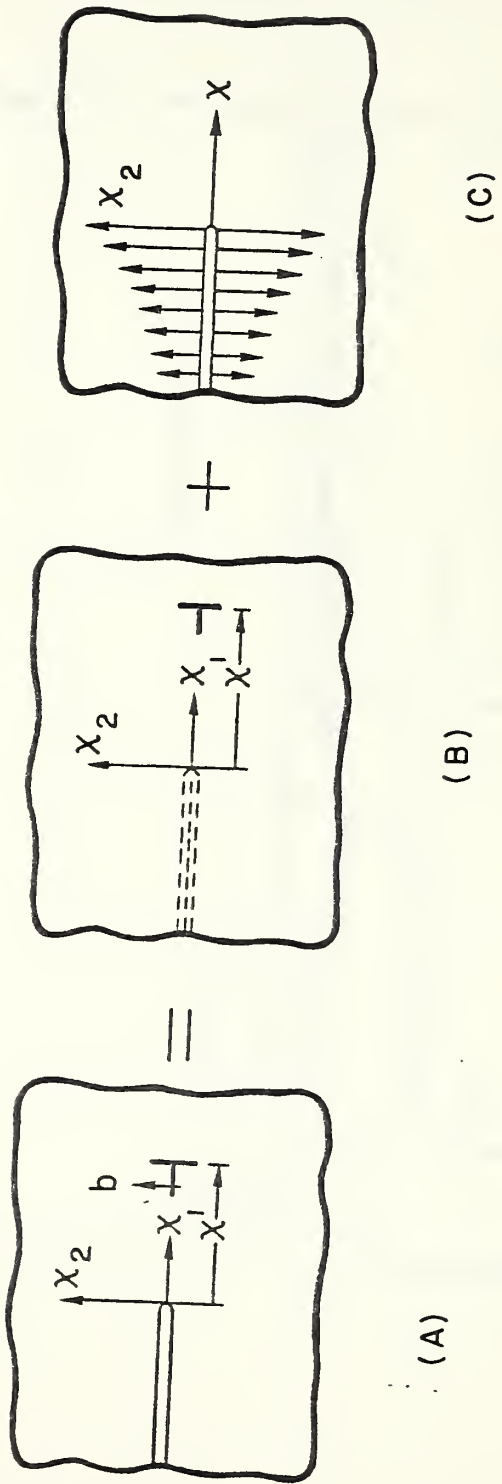


Fig 2

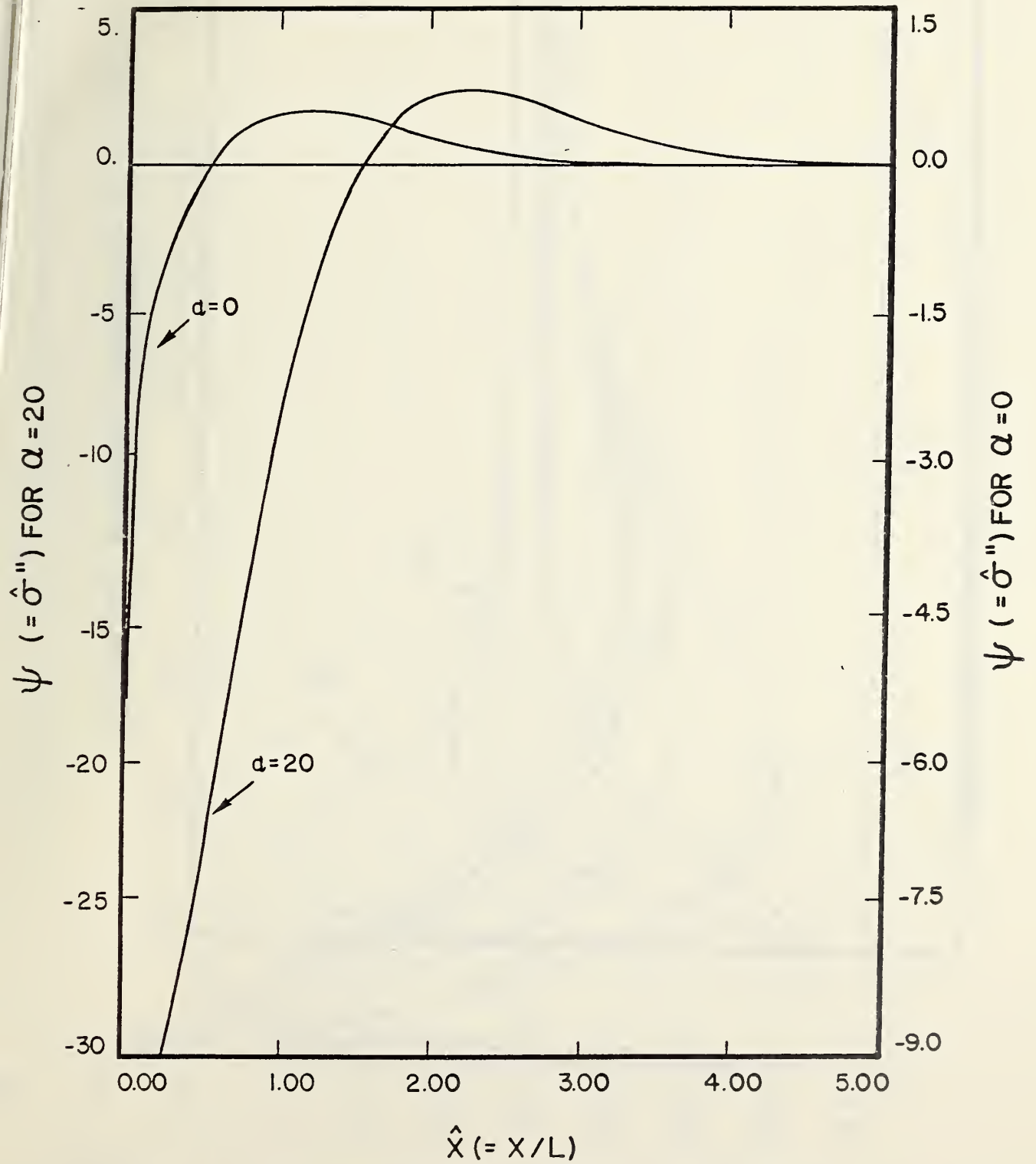


Fig 3

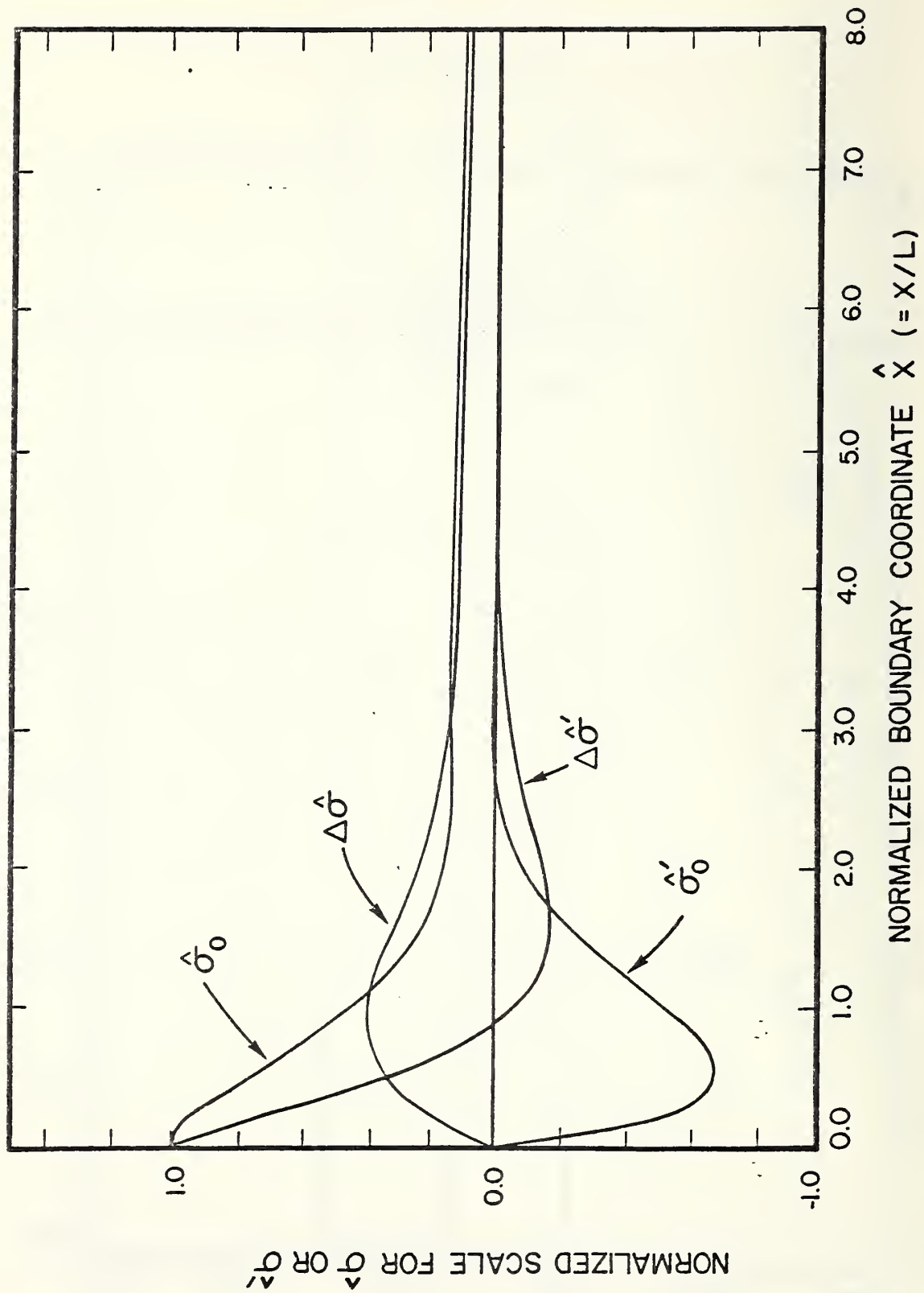


Fig 4

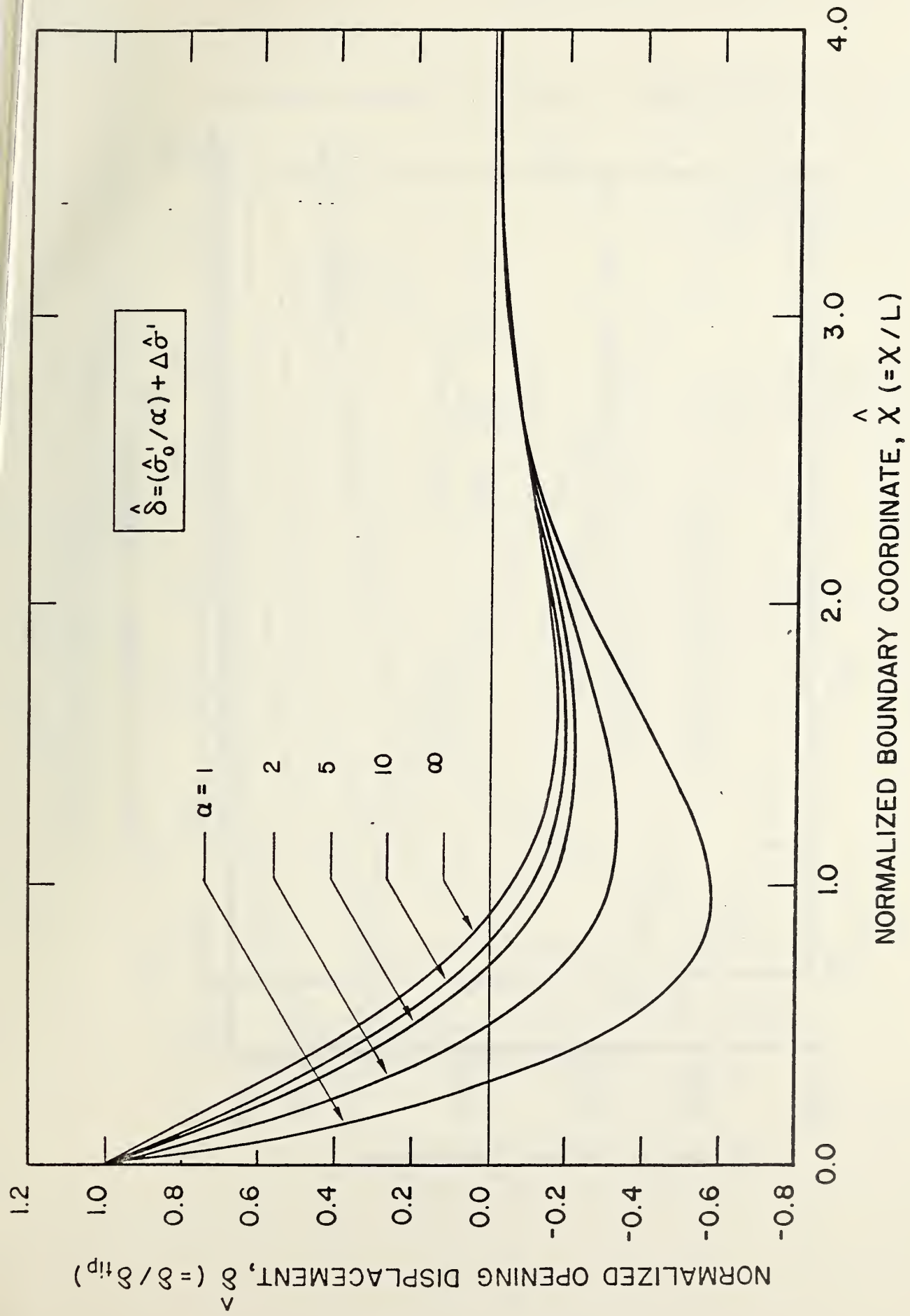


Fig 5

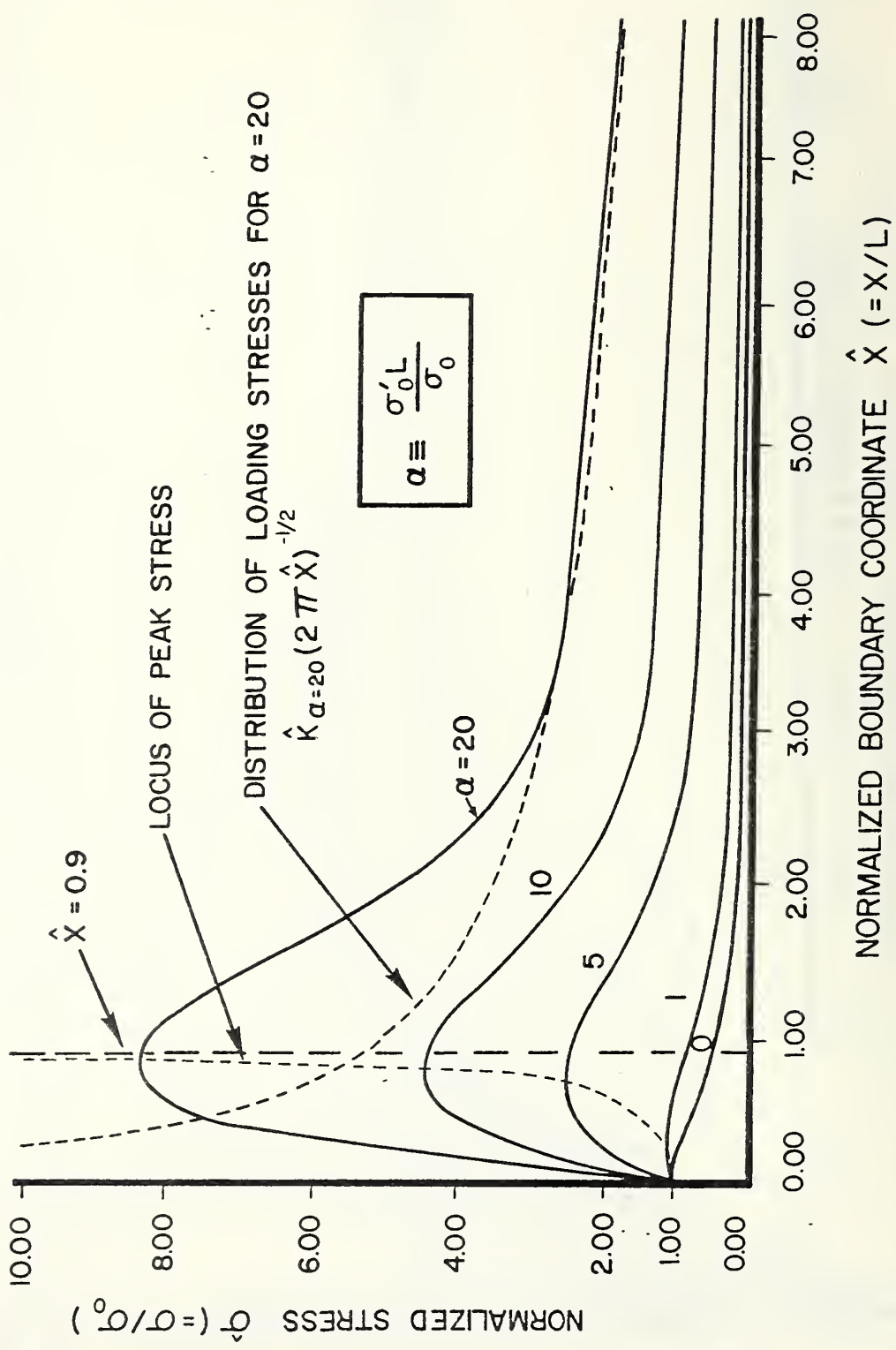


Fig 6

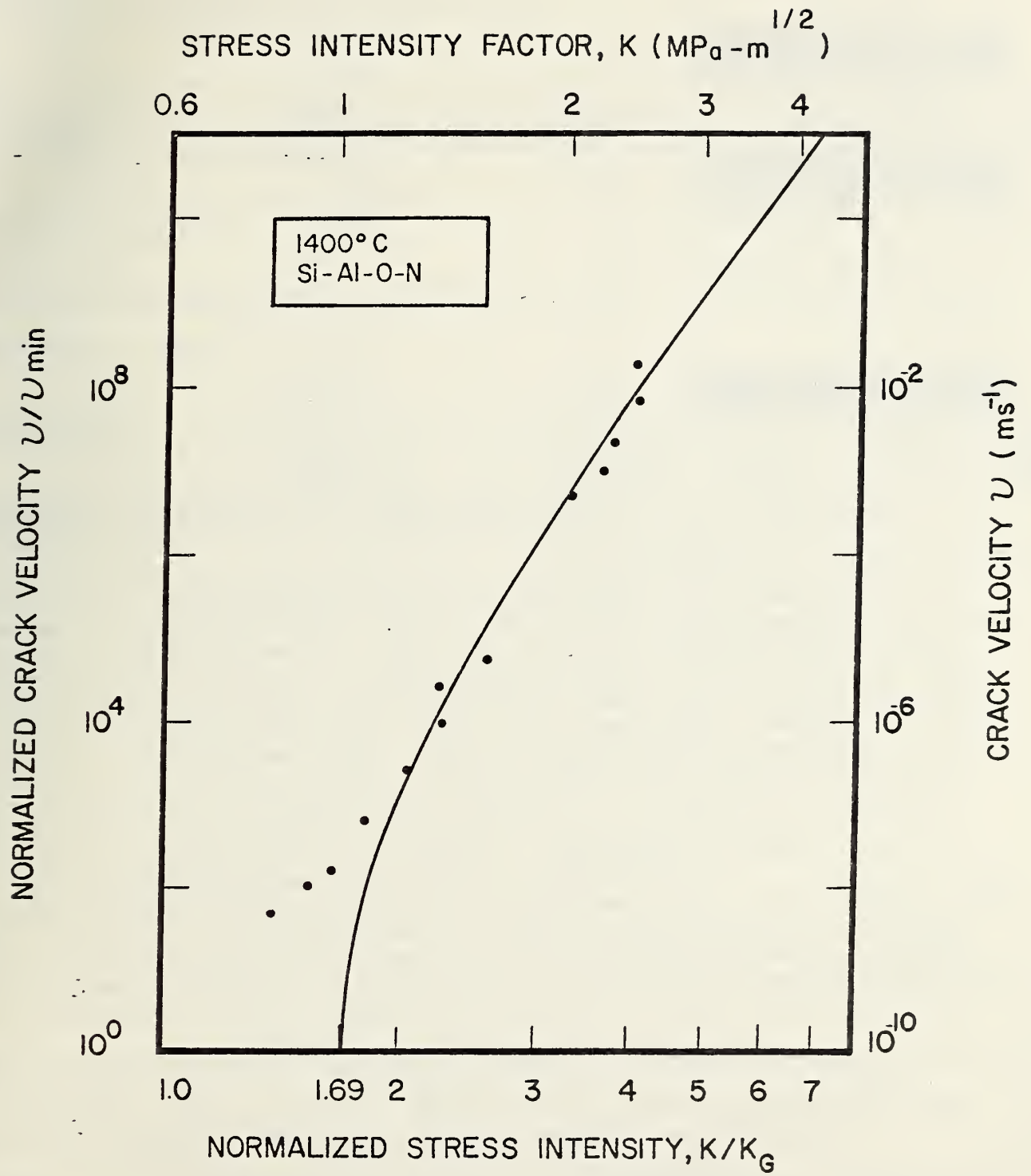


Fig 7

DEPT. OF COMM. BIOGRAPHIC DATA SHEET	1. PUBLICATION OR REPORT NO. NBS 81-2255	2. Gov't Accession No.	3. Recipient's Accession No.
4. TITLE AND SUBTITLE Diffusive Crack Growth Model for Creep Fracture		5. Publication Date March 1981	
		6. Performing Organization Code	
7. AUTHOR(S) Z-jer Chuang		8. Performing Organ. Report No.	
9. PERFORMING ORGANIZATION NAME AND ADDRESS NATIONAL BUREAU OF STANDARDS DEPARTMENT OF COMMERCE WASHINGTON, DC 20234		10. Project/Task/Work Unit No.	
		11. Contract/Grant No. DE-A105-800R 20679	
12. SPONSORING ORGANIZATION NAME AND COMPLETE ADDRESS (Street, City, State, ZIP) U.S. Department of Energy		13. Type of Report & Period Covered	
		14. Sponsoring Agency Code	
15. SUPPLEMENTARY NOTES			
<input type="checkbox"/> Document describes a computer program; SF-185, FIPS Software Summary, is attached.			
16. ABSTRACT (A 200-word or less factual summary of most significant information. If document includes a significant bibliography or literature survey, mention it here.) A grain boundary creep crack growth model is presented here based on the assumptions that the crack propagates along the grain boundary by a coupled process of surface and grain-boundary self-diffusion; the adjoining grains behave elastically; and steady state conditions prevail. Under the action of the applied stress, atoms at the crack surfaces are driven by surface diffusion toward the crack tip from where they are deposited non-uniformly by grain-boundary diffusion along the grain interface so that the grain boundary opens up in a wedge shape ahead of the advancing tip which in turn produces a misfit stress field. The total grain boundary stresses and opening displacements are solved from a system of integro-differential equations to give the following relating K to v : $(k/k_{min.}) = \frac{1}{2} [(v/v_{min.})^{1/12} + (v/v_{min.})^{-1/12}]$ where K is stress intensity factor and v the crack tip velocity. In terms of $v \propto K^n$, the equation predicts n varying from 12 to infinity. A comparison with data on Si-Al-O-N at 1400°C shows agreement between the theory and experiment. A consideration of the energy balance for the present model is also presented which indicates $J = (1-v^2)K^2/E$ is the correct energy release rate associated with the present crack growth model as is true in the theory of elastic fracture mechanics. However, the energy released in diffusion is in the form of work done by the normal stress along the grain boundary, not from the elastic strain energy loss of the adjoining grains.			
17. KEY WORDS (six to twelve entries; alphabetical order; capitalize only the first letter of the first key word unless a proper name; separated by semicolons) Crack growth model; Creep cavitation; Diffusive crack growth; Energy release rate; High temperature fracture; J-integral; Sialon; Singular integral equation			
18. AVAILABILITY <input checked="" type="checkbox"/> Unlimited <input type="checkbox"/> For Official Distribution. Do Not Release to NTIS <input type="checkbox"/> Order From Sup. of Doc., U.S. Government Printing Office, Washington, DC 20402, SD Stock No. SN003-003- <input type="checkbox"/> Order From National Technical Information Service (NTIS), Springfield, VA. 22161		19. SECURITY CLASS (THIS REPORT) UNCLASSIFIED	21. NO. OF PRINTED PAGES 58
		20. SECURITY CLASS (THIS PAGE) UNCLASSIFIED	22. Price \$8.00

